All Sciences Proceedings
http://as-proceeding.com/

5th International Conference on Applied Engineering and Natural Sciences

July 10-12, 2023 : Konya, Turkey

https://www.icaens.com/

Design and Assessment of the Solar Energy Based Direct Steam Generation Supercritical CO_2 Brayton Cycle

Serpil ÇELİK TOKER*[1], Önder KIZILKAN [1]

[1]*Mechanical Engineering/Isparta University of Applied Sciences, Turkey*

**serpilcelik@isparta.edu.tr*

Abstract – The aim of this study is to examine the performance of the supercritical CO_2 Brayton cycle (sCO_2-BC) with intercooling and reheating for low-temperature solar energy application. The heat required for the sCO_2-BC is supplied from an evacuated tube solar collector. Energy and exergy analyses of the solar energy-assisted sCO_2-BC with intercooling and reheating are investigated. In addition, the effects of operating parameters like solar radiation, collector number, compressor, and turbine input pressure on system performance are examined parametrically. According to the findings of the analysis, the net power production is found to be 0.2687 kW. In addition, the solar energy-based sCO_2-BC's energy and exergy efficiencies are found to be 3.68% and 3.95%, respectively. Moreover, it has been determined that the sCO_2-BC's energy and exergy efficiencies reduce with the increase of solar irradiation, the collector number, and the compressor inlet pressure, while the system's energy and exergy efficiencies rise with the increase of the turbine input pressure.

Keywords – Solar Energy, Evacuated Solar Collector, Supercritical CO_2 *Brayton Cycle, Energy, Exergy*

I. INTRODUCTION

Recently, energy demand has been rising rapidly due to industrialization, population growth, and high living standards. Utilizing fossil fuels for the majority of the earth's growing energy demands leads to the quick depletion of fossil fuel reserves, global warming, acid rain, and air pollution [1]. The usage of renewable energy resources like solar energy has become very important to reduce the problems caused by the usage of fossil fuels [2]. The useful energy obtained from the solar is easily utilized in the energy generation plants like the gas Brayton cycle [3], Rankine cycle [4], organic Rankine cycle [5], transcritical CO_2 Rankine cycle [6], and sCO_2-BC [7]. The sCO_2-BC has recently received a great deal of attention from research due to its advantages, such as high performance, compact turbomachinery, and environmentally friendly [8]. In addition, CO_2 is non-toxic, abundant in nature, inexpensive, and it is not flammable. Moreover, the global warming potential (GWP) of CO_2 is 1, and its ozone depletion potential (ODP) is 0 [9]. Wang et al. (2018) investigated the performances of five different sCO_2-BCs, solar tower-assisted partial cooling, recompression, precompression, intercooling, and recuperation. They stated that the highest performance was in the sCO_2-BC with intercooling, and the lowest performance was in the sCO_2-BC with recuperation [10]. Wang and He (2017) performed performance of the solar energy-based recompression sCO_2-BC [11]. Cao et al. (2022) studied the thermodynamic analyses of the solar assisted five different sCO_2-BCs including precompression, recompression, intercooling and partial cooling [12]. Liang et al. (2020) done the optimization of the cycles by making thermodynamic analyzes of the sCO_2-BC and organic Rankine cycle combined with the solar tower [13]. The performance of five various (simple, recuperator, recompression, pre-compression, and split expansion) sCO_2-BCs with solar energy were conducted by Al-Sulaiman and Atif (2015) [14].

As mentioned above, there are many studies in the literature on sCO$_2$-BCs used for high-temperature solar energy applications such as solar towers and parabolic solar collectors. In addition to high-temperature applications, it is very important to ensure energy conversion from low-temperature applications. Studies on evacuated solar collectors based on sCO$_2$-BC used for low-grade solar energy applications are limited. For this purpose, thermodynamic analysis of the evacuated solar collector-assisted sCO$_2$-BC was performed in this paper. In addition, parametric studies were carried out according to the main factors affecting the system performance, such as solar radiation, number of collectors, compressor, and turbine inlet pressure.

II. SYSTEM DESCRIPTION AND THERMODYNAMIC ANALYSIS

Fig. 1 presents the configuration of the solar energy-assisted sCO$_2$-BC with intercooling and reheating. The solar energy-based plant comprises an evacuated solar collector, compressor, turbine, intercooler, recuperator, and gas cooler. The heat required for the sCO$_2$-BC is supplied from the evacuated solar collector. In sCO$_2$-BC with intercooling and reheating, the intercooling and reheating process reduces compressor work and increase turbine work, respectively.

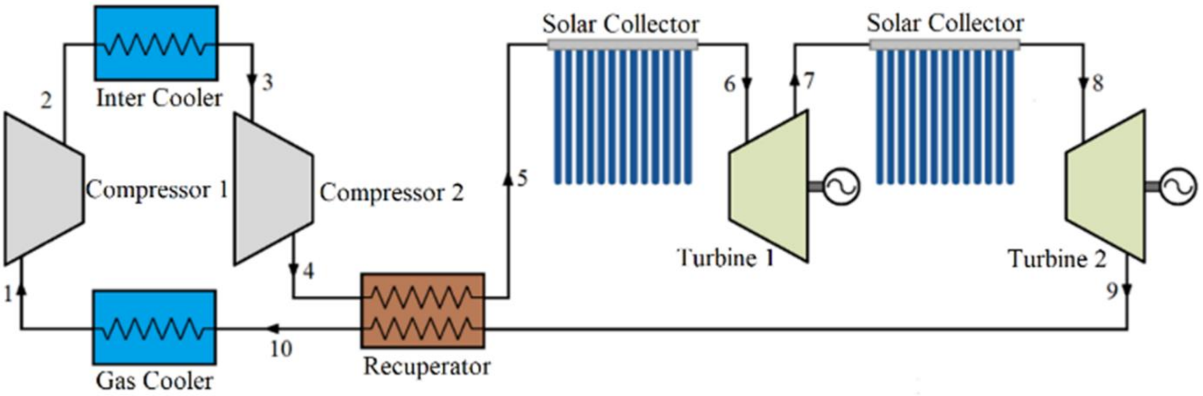

Fig. 1. Solar energy-based sCO$_2$-BC with intercooling and reheating

The system's initial parameters given in Table 1 were used in the solar energy-assisted sCO$_2$-BC's thermodynamic analysis. Energy and exergy analyses are performed utilizing the EES program for the integrated system's performance assessment. In this study, the thermodynamic analysis is made under the following assumptions:

- It is supposed that the plant is operating in a steady state.
- Kinetic and potential energies can be neglected.
- The compressor and turbine processes are thought to be adiabatic.
- The reference state properties are 20 °C and 101.325 kPa.

Table 1. Operating parameters of solar energy-based sCO$_2$-BC

Parameter	Value
Turbine input pressure	15000 kPa
Compressor input pressure	8000 kPa
Solar radiation	600 W/m^2
Compressor inlet temperature	32 °C
Isentropic compressor's efficiency	86
Isentropic turbine's efficiency	86
Recuperator effectiveness	55

The useful heat energy obtained from the evacuated solar collector can be found as follows:

$$\dot{Q}_u = F_R\, I_{solar}\, A_{ri} - F_R A_r U_L (T_{in} - T_a) \qquad (1)$$

Here, F_R is collector heat removal factor, I_{solar} is the solar irradiation, A_{ri} is the projection area of the absorber tube, A_r is the absorber tube area, U_L is the entire heat loss coefficient of the collector between the ambient and absorber tube, T_{in} is the collector input temperature of the working agent and T_a is the atmospheric temperature. F_R is determined from the following equation:

$$F_R = \frac{\dot{m}c_p}{A_r U_L}\left[1 - \exp\left(-\frac{U_L F' A_r}{\dot{m}c_p}\right)\right] \qquad (2)$$

Here, cp, ṁ, and F are the fluid's specific heat, agent's mass current rate, and collector efficiency factor, respectively. Also, the beneficial heat gain can be calculated by the formula:

$$\dot{Q}_u = \dot{m}c_p(T_{out} - T_{in}) \tag{3}$$

where, T_{out} is the agent output temperature.

The mass, energy, entropy, and exergy balance equations can be defined following as:

$$\sum \dot{m}_{in} = \sum \dot{m}_{out} \tag{4}$$

$$\dot{Q} + \sum \dot{m}_{in}h_{in} = \dot{W} + \sum \dot{m}_{out}h_{out} \tag{5}$$

$$\sum \dot{m}_{in}s_{in} + \sum \frac{\dot{Q}}{T} + \dot{S}_{gen} = \sum \dot{m}_{out}s_{out} \tag{6}$$

$$\dot{E}x_Q - \dot{E}x_W = \sum \dot{m}_{out}e_{out} - \sum \dot{m}_{in}e_{in} + \dot{E}x_{dest} \tag{7}$$

here, $\dot{Q}$ is the heat rate, $\dot{W}$ is the work rate, h is the specific enthalpy, s is the specific entropy, $\dot{S}_{gen}$ is the entropy production, e is the flow exergy, and $\dot{E}x_{dest}$ is the exergy irreversibility. The solar energy-based sCO_2-BC's energy and exergy efficiencies are computed with the following:

$$\eta_{en} = \frac{\dot{W}_{net}}{I_{solar}\ A_{ri}} \tag{8}$$

$$\eta_{ex} = \frac{\dot{W}_{net}}{\dot{E}x_{solar}} \tag{9}$$

III. RESULTS AND DISCUSSION

Thermodynamic analysis of the solar energy-based sCO_2-BC with intercooling and reheating is conducted considering steady-state conditions. The impact of solar irradiation on net power and the cycle's energy efficiency is shown in Fig. 2. With the rise in solar radiation, the amount of net power generation raised continuously, while the cycle's energy efficiency increased up to 600 W/m^2 of solar irradiation and then reduced. The reason for the diminish in energy efficiency is that the amount of increase in net power according to solar radiation is less than the amount of thermal power falling on the solar collector.

Fig. 3 displays the cycle's exergy irreversibility and the cycle's exergy efficiency relative to solar radiation. As the solar radiation value increases, the exergy destruction rises while the exergy efficiency reduces. As the exergy destruction of the solar collector rises with the increase in the amount of solar irradiation, the system's total exergy destruction expands.

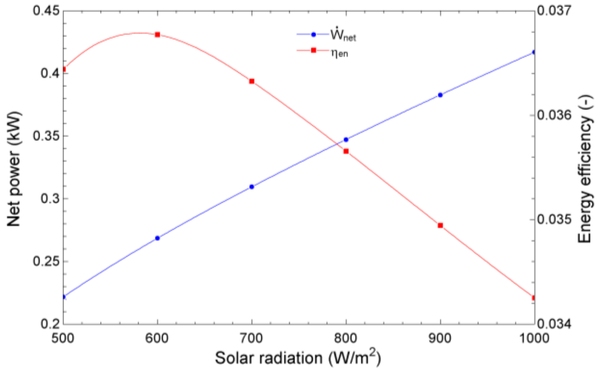

Fig. 2. Variation of net power and energy efficiency with respect to solar radiation

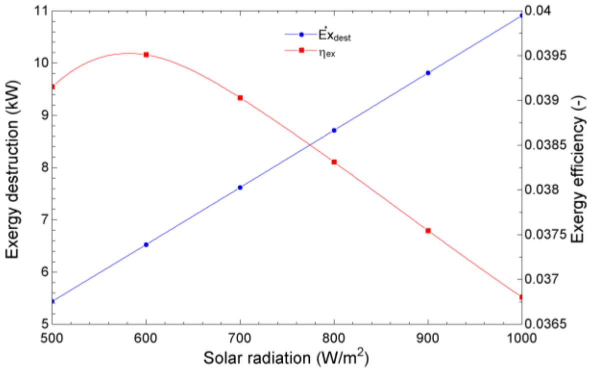

Fig. 3. Variation of exergy destruction and exergy efficiency with respect to solar radiation

Fig. 4 exhibits the alteration of the net power and the cycle's energy efficiency according to the total collector number in the sCO_2-BC with intercooling and reheating. With the increase in the total collector number from 10 to 25, the net power produced from the cycle rises from 0.249 kW to 0.281 kW, while the cycle's energy efficiency reduces from 4.5% to 2.5%. The reason for the decrease in the energy efficiency is that with the increase of collector number, the thermal power falling on the collector rises more than the net power. The effect of the total collector number on exergy irreversibility and exergy efficiency is shown in Fig. 5. With the rise in the total collector number, the exergy destruction of the cycle expands while the cycle's exergy efficiency decreases. With the increment in the number collector from 10 to 25, exergy destruction raises from 4.84 kW to 9.91 kW, while the system's exergy efficiency diminishes from 4.88% to 2.75%.

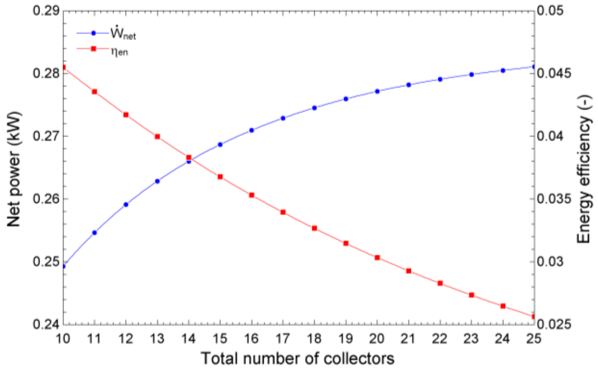

Fig. 4. Variation of net power and energy efficiency according to the total collector number

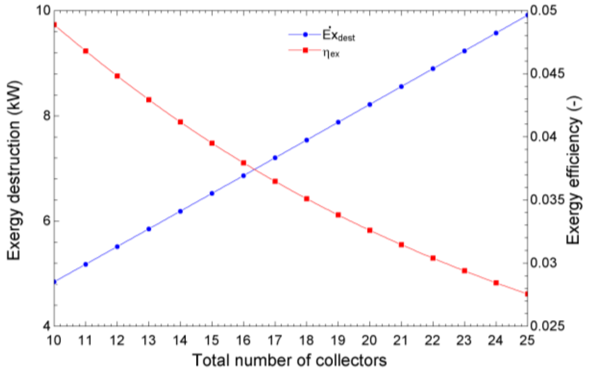

Fig. 5. Variation of exergy destruction and exergy efficiency according to the total collector number

The impact of compressor input pressure on net power and energy efficiency is shown in Fig. 6, and its effect on exergy irreversibility and exergy efficiency is represented in Fig. 7. Since the increment in compressor inlet pressure causes a reduction in net power, the cycle's energy and exergy efficiencies also reduces. As the compressor inlet pressure rises from 8000 kPa to 13000 kPa, the cycle's exergy destruction increases from 6.52 kW to 6.73 kW, while the cycle's exergy efficiency diminishes from 3.7% to 1.0%.

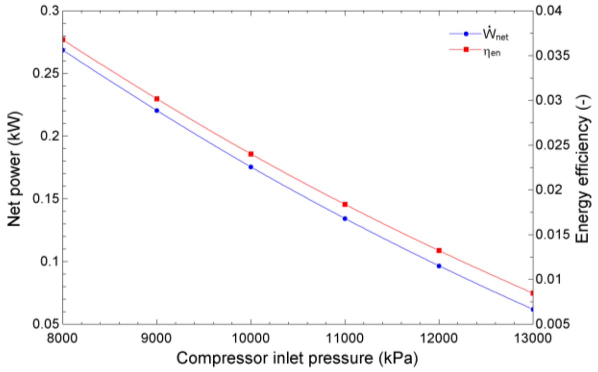

Fig. 6. Variation of net power and energy efficiency according to the compressor input pressure

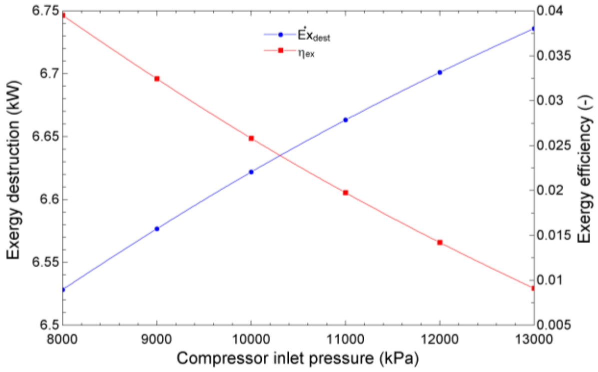

Fig. 7. Variation of exergy destruction and exergy efficiency according to the compressor inlet pressure

Fig. 8 shows the change in net power and energy efficiency with respect to turbine input pressure, while Fig. 9 indicates the effect of turbine input pressure on exergy destruction and exergy efficiency. With the turbine input pressure growing from 15000 kPa to 20000 kPa, the net power rises from 0.268 kW to 0.321 kW, while the energy efficiency of the cycle increases from 3.67% to 4.39%. In addition, as the turbine input pressure increases, the exergy irreversibility in the cycle reduces while the exergy efficiency of the cycle rises.

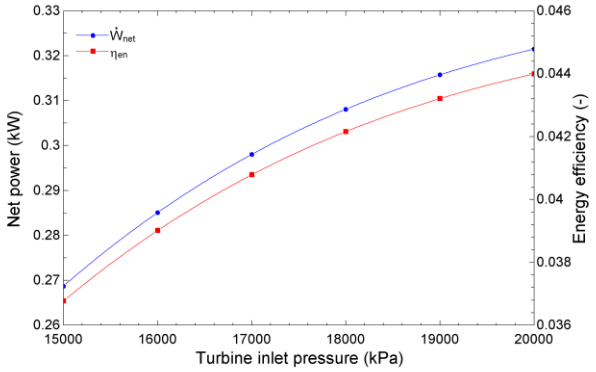

Fig. 8. Variation of net power and energy efficiency according to the turbine input pressure

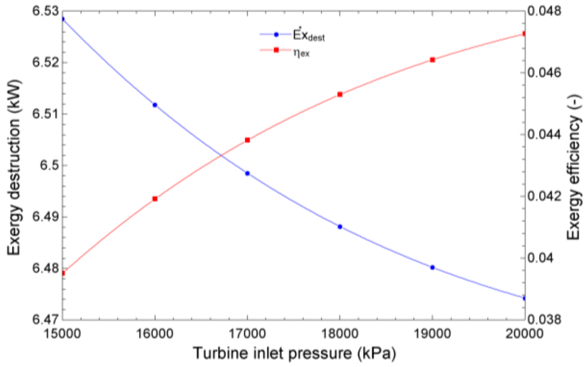

Fig. 9. Variation of exergy destruction and exergy efficiency according to the turbine input pressure

IV. CONCLUSION

In this study, the performance of solar energy assisted sCO_2-BC with intercooling and reheating using EES software. The key results of this paper are as follows:

- The net power generated from the sCO_2-BC with intercooling and reheating is 0.2687 kW, and the heat entering the cycle is 7.308 kW.
- The energy and exergy efficiencies of the solar energy-assisted sCO_2-BC with intercooling and reheating are calculated as 3.68% and 3.95%, respectively.
- The exergy destruction of the integrated system was found to be 6.53 kW.
- The energy and exergy efficiencies of sCO_2-BC are reduced with increasing solar radiation and collector number.

REFERENCES

[1] A. Khaliq, E. M. A. Mokheimer, and M. Yaqub, "Thermodynamic investigations on a novel solar powered trigeneration energy system," *Energy Convers. Manag.*, vol. 188, pp. 398–413, May 2019.

[2] O. Kizilkan and H. Yamaguchi, "Feasibility research on the novel experimental solar-assisted CO_2 based Rankine cycle integrated with absorption refrigeration," *Energy Convers. Manag.*, vol. 205, p. 112390, Feb. 2020.

[3] G. Gavagnin, D. Sánchez, G. S. Martínez, J. M. Rodríguez, and A. Muñoz, "Cost analysis of solar thermal power generators based on parabolic dish and micro gas turbine: Manufacturing, transportation and installation," *Appl. Energy*, vol. 194, pp. 108–122, May 2017.

[4] X. Shi, J. Song, Q. He, Y. Liu, H. Fu, and S. Cui, "A novel liquefied air energy storage system with solar energy and coupled Rankine cycle and seawater desalination," *J. Energy Storage*, vol. 61, p. 106759, May 2023.

[5] Y. Li, S. Teng, and H. Xi, "3E analyses of a cogeneration system based on compressed air energy storage system, solar collector and organic Rankine cycle," *Case Stud. Therm. Eng.*, vol. 42, p. 102753, Feb. 2023.

[6] J. Meng, M. Wei, P. Song, R. Tian, L. Hao, and S. Zheng, "Performance evaluation of a solar transcritical carbon dioxide Rankine cycle integrated with compressed air energy storage," *Energy Convers. Manag.*, vol. 215, p. 112931, Jul. 2020.

[7] Y. Tong, L. Duan, Y. Jiang, M. Yang, and L. Pang, "Performance study of a novel supercritical CO_2 solar-coal supplementary power generation system," *Appl. Therm. Eng.*, vol. 218, p. 119375, Jan. 2023.

[8] Y. Ahn *et al.*, "Review of supercritical CO_2 power cycle technology and current status of research and development," *Nucl. Eng. Technol.*, vol. 47, no. 6, pp. 647–661, Oct. 2015.

[9] S. Gharehdaghi, S. F. Moujaes, and A. Mahdavi Nejad, "Thermal-fluid analysis of a parabolic trough solar collector of a direct supercritical carbon dioxide Brayton cycle: A numerical study," *Sol. Energy*, vol. 220, pp. 766–787, May 2021.

[10] K. Wang, M. J. Li, J. Q. Guo, P. Li, and Z. Bin Liu, "A systematic comparison of different S-CO_2 Brayton cycle layouts based on multi-objective optimization for applications in solar power tower plants," *Appl. Energy*, vol. 212, pp. 109–121, Feb. 2018.

[11] K. Wang and Y. L. He, "Thermodynamic analysis and optimization of a molten salt solar power tower integrated with a recompression supercritical CO_2 Brayton cycle based on integrated modeling," *Energy Convers. Manag.*, vol. 135, pp. 336–350, Mar. 2017.

[12] Y. Cao, P. Li, Z. Qiao, S. Ren, and F. Si, "A concept of a supercritical CO_2 Brayton and organic Rankine combined cycle for solar energy utilization with typical geothermal as auxiliary heat source: Thermodynamic analysis and optimization," *Energy Reports*, vol. 8, pp. 322–333, Nov. 2022.

[13] Y. Liang, J. Chen, X. Luo, J. Chen, Z. Yang, and Y. Chen, "Simultaneous optimization of combined supercritical CO_2 Brayton cycle and organic Rankine cycle integrated with concentrated solar power system," *J. Clean. Prod.*, vol. 266, p. 121927, Sep. 2020.

[14] F. A. Al-Sulaiman and M. Atif, "Performance comparison of different supercritical carbon dioxide Brayton cycles integrated with a solar power tower," *Energy*, vol. 82, pp. 61–71, Mar. 2015.

[15] I. Dincer and M. A. Rosen, “Exergy and Energy Analyses,” *Exergy*, pp. 21–30, Jan. 2013.